

## Ultrafast carrier dynamics and saturable absorption of solution-processable few-layered graphene oxide

Xin Zhao,<sup>1</sup> Zhi-Bo Liu,<sup>1,a)</sup> Wei-Bo Yan,<sup>2</sup> Yingpeng Wu,<sup>2</sup> Xiao-Liang Zhang,<sup>1</sup>  
Yongsheng Chen,<sup>2,a)</sup> and Jian-Guo Tian<sup>1</sup>

<sup>1</sup>Key Laboratory of Weak Light Nonlinear Photonics, Ministry of Education, Teda Applied Physics School, School of Physics, Nankai University, Tianjin 300457, People's Republic of China

<sup>2</sup>Key Laboratory for Functional Polymer Materials and Centre for Nanoscale Science and Technology, Institute of Polymer Chemistry, College of Chemistry, Nankai University, Tianjin 300071, People's Republic of China

(Received 7 January 2011; accepted 3 March 2011; published online 22 March 2011)

Ultrafast carrier dynamics and saturable absorption of few-layered graphene oxide, well-dispersed in organic solvent, are studied using femtosecond pump-probe and Z-scan techniques. The results demonstrate that few-layered graphene oxide has a fast energy relaxation of hot carriers and strong saturable absorption, which is comparable with that of reduced graphene oxide. Fast carrier relaxation combined with well solution processing capability arises from the large fraction of  $sp^2$  carbon atom inside the few-layered graphene oxide sheet together with oxidation mainly existing at the edge areas. This superiority of few-layered graphene oxide will facilitate potential applications of graphene for ultrafast photonics. © 2011 American Institute of Physics. [doi:10.1063/1.3570640]

Graphene, as a two-dimensional carbon nanomaterial, shows remarkable optical properties and has potential applications in photonics and optoelectronics.<sup>1</sup> For example, the ultrafast carrier dynamics, combined with large absorption and Pauli blocking, make graphene an ideal ultrabroadband and fast saturable absorber in the application of ultrafast laser.<sup>2–4</sup> The ultrafast dynamics of charge carriers in graphene have been reported using ultrafast pump-probe technique, and fast decay times from tens to hundreds of femtosecond were assigned to carrier–carrier scattering and carrier–phonon scattering.<sup>5–7</sup> However, it is known that the solubility and/or processability are the first issue for many perspective applications of graphene-based materials. For this reason, chemical exfoliation methods which produce graphene oxide (GO) from graphite are developed and result in high-yield production of single sheet dispersions. Unfortunately, carbon atoms bonded with oxygen groups are  $sp^3$  hybridized and disrupt the  $sp^2$  conjugation of the hexagonal graphene lattice in GO, and thus destroy the linear dispersion of the Dirac electrons and influence the unique optical properties of graphene.<sup>8,9</sup> For example, this will make GO unsuitable as a broadband saturable absorber in laser cavities for ultrafast pulse generation.<sup>10</sup> Is it possible for us to improve the solubility and preserve some of unique properties of the pristine material simultaneously? For this purpose, we studied ultrafast carrier dynamics and saturable absorption of few-layered GO (FGO), which can be well-dispersed in organic solvent. The fast carrier relaxation and large saturable absorption of FGO in *N,N*-dimethylmethanamide (DMF) solution indicate that oxidation mainly exists at the edge areas and has ignorable effect on ultrafast dynamics and optical nonlinearities. The solution-processability and fast nonlinear response of FGO offer unique advantage since it is readily amenable by spin-coating, spray-casting, drop-casting, or

inkjet printing onto substrates for large-scale production of graphene optoelectronics.

FGO used in our experiments was synthesized by arc-discharge method using a buffer gas containing carbon dioxide.<sup>11</sup> It can be well dispersed in common organic solvents. Based on an atomic force microscopy (AFM) statistical height analysis, the distribution of FGO is mainly four to five layers with layer size of about 100–300 nm.<sup>11</sup> The x-ray photoelectron spectroscopy and x-ray diffraction indicate that the relative content of the nonoxygenated  $sp^2$  carbon atoms is much higher than that in conventional GO using chemical methods, and most of the disordered oxidation domains exist at the edge areas.<sup>11</sup> FGO was dispersed in DMF with concentration of 0.2 mg/ml and filled in a 2-mm-thick quartz cell. For comparison, we also prepared GO suspension in DMF and reduced GO (RGO) film. GO was prepared from purified natural graphite according to a modified hummer method,<sup>12</sup> and also dispersed in DMF with concentration of 0.2 mg/ml. GO film was first produced by a spin-coating method using GO solution on the quartz substrate. And then, GO film was reduced through exposure to hydrazine vapor and succedent anneal in 1000 °C. Finally, RGO with a thickness of less than twenty nanometers was obtained by reduction in GO film.

Figure 1 shows the ultraviolet-visible-near infrared (UV-vis-NIR) absorption (a), photoluminescence (b), and Raman (c) spectra of FGO and GO suspensions and RGO film. The absorption increasing of GO from the near infrared to ultraviolet is faster than that of FGO and RGO due to different  $\pi$ -electron concentration and structural ordering.<sup>9</sup> FGO shows a broadband absorption in the whole spectral region like RGO. For GO, localized  $sp^2$  clusters are isolated by large scale of  $sp^3$  fractions and broad photoluminescence [Fig. 1(b)] suggests a dispersion of hard gaps.<sup>13</sup> No photoluminescence was observed in FGO and RGO, indicating there are little localized electronic states because of the large scales of  $sp^2$  conjugation in FGO and RGO. This is consis-

<sup>a)</sup>Authors to whom correspondence should be addressed. Electronic addresses: rainingstar@nankai.edu.cn and yschen99@nankai.edu.cn.

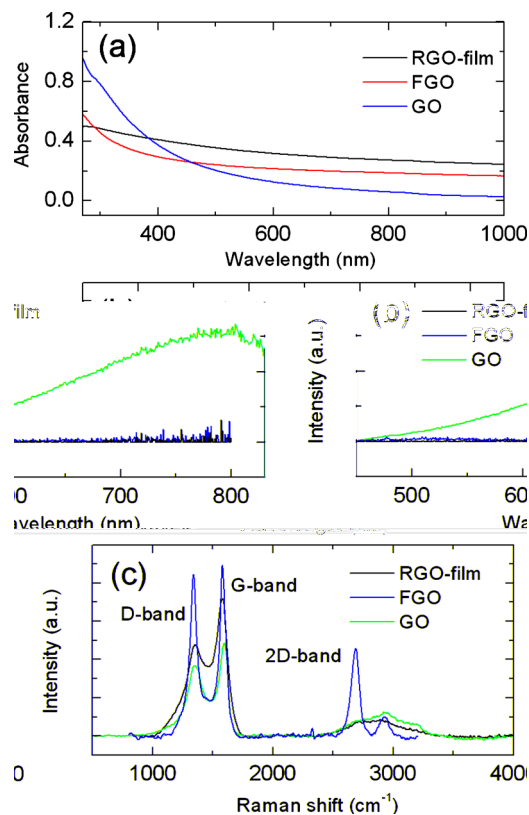


FIG. 1. (Color online) UV-vis-NIR absorption (a), photoluminescence (b), and Raman (c) spectra of FGO, GO suspensions and RGO film.

tent with pure graphene in which fluorescence is not existent due to large fraction of  $sp^2$  carbon atom.<sup>14</sup>

The sharp and high G peak of FGO in Raman spectra [Fig. 1(c)] arises from bond stretching of  $sp^2$  carbon pairs in both aromatic rings and chains. The G peak (1580  $\text{cm}^{-1}$ ) is shifted to higher frequencies with respect to that of RGO-film (1582  $\text{cm}^{-1}$ ) and GO (1598  $\text{cm}^{-1}$ ), implying less doping defects.<sup>15</sup> High and sharp 2D peak also indicates FGO has a better order than RGO and GO.<sup>9</sup> The intensity ratio of the G peak to that of the 2D peak ( $I_G/I_{2D}$ ) has a good correlation with the number of graphene layers present. The  $I_G/I_{2D} \approx 2$  in FGO is larger to the value for three layers graphene ( $I_G/I_{2D} \sim 1.3$ ),<sup>16</sup> which is identical to the results of four to five layers obtained from AFM. The ratio  $I_G/I_D$  is related to the in-plane crystallite size, thus it is expected that a larger ratio  $I_G/I_D$  should be in FGO due to its less defects than GO. However, we found that our FGO shows a ratio  $I_G/I_D$  of 1.06, smaller than that of GO ( $I_G/I_D = 1.32$ ) and RGO ( $I_G/I_D = 1.48$ ). We believe that the smaller  $I_G/I_D$  of FGO should be associated with the number of layers, because the D-band not only arises from disorder but also increases in intensity with the number of layers.<sup>17</sup>

Degenerate pump-probe experiment was carried out using femtosecond laser pulses from a Ti:sapphire laser amplifier (1 K Hz, Spitfire, Spectra Physics) at 800 nm with the pulse duration of 130 fs. The pump pulse was modulated at 383 Hz with the help of an optical chopper, the probe pulse was delayed and the transmitted probe pulse was sent to one photodiode of a balanced detector, which was connected to a lock-in amplifier referenced to the optical chopper. The intensity of pump and probe beam were 18  $\text{GW}/\text{cm}^2$  and

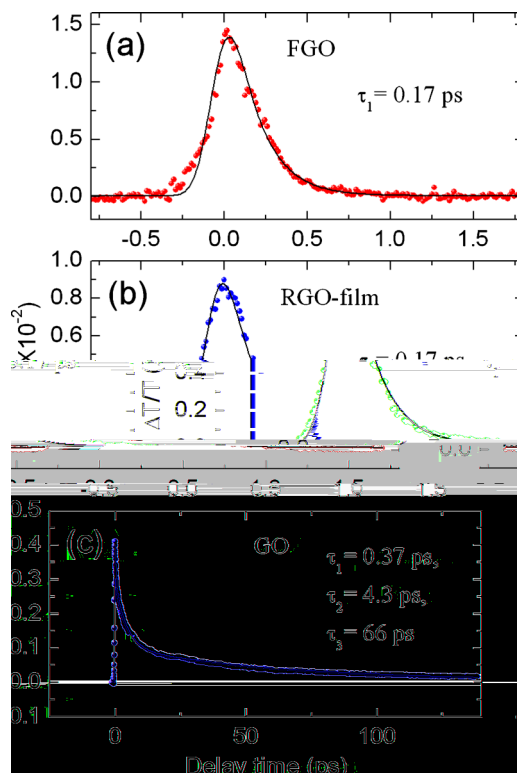


FIG. 2. (Color online) Transient differential transmission spectra of the FGO and GO suspensions and RGO film as a function of probe delay in degenerate pump-probe experiments at 800 nm: (a) FGO in DMF, (b) RGO film, and (c) GO in DMF. The solid lines are fittings to mono-exponentially decaying functions (FGO and RGO) and tri-exponential response function (GO) convoluted with the cross correlation of the pump and probe pulses.

1.6  $\text{GW}/\text{cm}^2$ , respectively. The polarization of pump was parallel to that of probe beam.

Figure 2 gives the transient differential transmission spectra for the FGO and GO suspensions and RGO film. The pump-induced change in transmission is dominated by absorption saturation in three samples, resulting in a positive differential transmission  $\Delta T/T_0 = (T - T_0)/T_0$ .  $T$  and  $T_0$  are the sample transmissions with and without excitation, respectively. The data was fitted using an exponentially decaying function,  $\Delta T/T_0 = \sum_i A_i \exp(-t/\tau_i)$ , convoluted with the cross correlation of the pump and probe pulses.

Since most fraction of  $sp^2$ -hybridized domains inside FGO remains during oxidation process and oxygen-containing functional groups locate at the edges, the structure of interlayer spacing inside FGO is similar to that of normal graphite. Therefore, it is expected that in FGO there is a fast decay time like the pristine graphene because the photoinduced bleaching only occurs in  $sp^2$ -hybridized domains. From Fig. 2, we can see that the decay trend of FGO and RGO are comparable and the fast decay time  $\tau$  of FGO is also about 0.17 ps. The result of fast decay time  $\tau$  in FGO is in agreement with those of 0.14 ps in Ref. 5 and 0.09–0.18 ps in Ref. 7. This fast decay time of FGO is considered to arise from carrier-phonon scattering, just like RGO. The faster carrier-carrier scattering could be not resolved in our experiments since its response time is within few tens of femtosecond. The result of pump-probe measurement (Fig. 2) in FGO is consistent with our hypothesis that the oxidation at the edges has weak influence on ultrafast carrier dynamics of graphene.

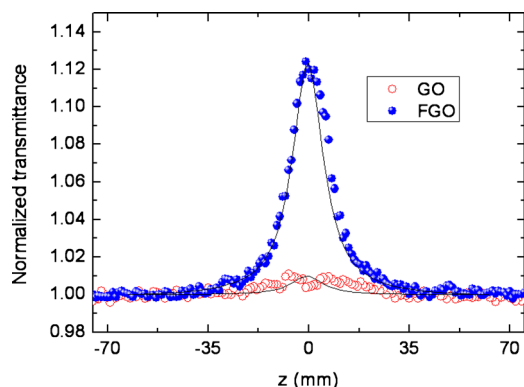


FIG. 3. (Color online) Open-aperture Z-scan curves of FGO (filled circles) and GO (open circles). The solid lines are theoretical fittings.

Compared with GO ( $\tau_1=0.37$  ps), in which oxidation exist in both the surface and edge, this edge-oxidation material FGO has shorter carrier-phonon scattering time (0.17 ps). It can arise from the larger carrier density in FGO than in GO. For GO, two fast time constants of  $\tau_1=0.37$  ps and  $\tau_2=4.3$  ps reflect the carrier intraband relaxation processes of carrier-optical phonon scattering and carrier-acoustic phonon scattering. However, the major difference between the carrier dynamics in GO and FGO is the slow third time constant of  $\tau_3=67$  ps, which was not observed in most of reports on graphene yet. The presence of energy band gap related to the size of the nanometer-scale  $sp^2$  clusters in GO, leads to a slow interband carrier recombination after excited in GO, so that the possible origin of  $\tau_3$  in GO is slow interband carrier recombination. Despite the fact that GO has well solution processing capability, a consequence of  $sp^3$ -hybridized carbon by oxygen-containing functional groups in GO is that some of unique properties of the pristine graphene will be limited, such as the fast relaxation responsible that is a key parameter in the application of ultrafast photonics. Compared with GO, graphene is more suitable as saturable absorber in ultrafast fiber laser owing to its fast decay time and wideband strong IR absorbance.<sup>10</sup>

Z-scan technique was used to measure their saturable absorption,<sup>18</sup> and their Z-scan curves are shown in Fig. 3, where the on-axis peak intensity is  $77.5$  GW/cm<sup>2</sup>. The Z-scan curves exhibit a peak with respect to the focus, indicating that saturable absorption exists for FGO and GO due to photoinduced bleaching. The absorption coefficient in the case of two-level system possessing inhomogeneously broadened states can be written as  $\alpha=\alpha_0/(1+I/I_S)^{0.5}$ ,<sup>19</sup> where  $\alpha_0$  is linear absorption coefficient,  $I$  is laser intensity, and  $I_S$  is saturable intensity. Linear absorption coefficients of GO and FGO in DMF at 800 nm are  $0.62$  cm<sup>-1</sup> and  $10.6$  cm<sup>-1</sup>, respectively. The solid lines in Fig. 3 are the theoretical fits with  $I_S=5.5\times 10^{10}$  W/cm<sup>2</sup> for FGO and  $I_S=13\times 10^{10}$  W/cm<sup>2</sup> for GO. Hence, it can be seen from Fig.

3 that FGO has stronger saturable absorption than GO. We have checked that the pump-probe and Z-scan experiments carried out on the pure solvent of DMF did not show any response under the same experimental conditions.

In summary, ultrafast carrier dynamic and saturable absorption of solution-processable FGO have been demonstrated using degenerate pump-probe and Z-scan techniques at 800 nm. This material has not only good solution processing capability but also excellent properties of the pristine graphene owing to oxidation at the edges. This makes it a good candidate for uses in applications of ultrafast photonics and optical switching.

This research was supported by Chinese National Key Basic Research Special Fund (Grant No. 2011CB922003), Natural Science Foundation of China (Grant Nos. 10974103 and 50933003), the Program for New Century Excellent Talents in University (Grant No. NCET-09-0484), the Natural Science Foundation of Tianjin (Grant No. 09JCYBJC04300), and the Key Project of Chinese Ministry of Education (Grant No. 109039).

- <sup>1</sup>F. Bonaccorso, Z. Sun, T. Hasan, and A. C. Ferrari, *Nat. Photonics* **4**, 611 (2010).
- <sup>2</sup>Z. P. Sun, T. Hasan, F. Torrisi, D. Popa, G. Privitera, F. Q. Wang, F. Bonaccorso, D. M. Basko, and A. C. Ferrari, *ACS Nano* **4**, 803 (2010).
- <sup>3</sup>Q. L. Bao, H. Zhang, Y. Wang, Z. H. Ni, Y. L. Yan, Z. X. Shen, K. P. Loh, and D. Y. Tang, *Adv. Funct. Mater.* **19**, 3077 (2009).
- <sup>4</sup>H. Zhang, D. Y. Tang, R. J. Knize, L. M. Zhao, Q. L. Bao, and K. P. Loh, *Appl. Phys. Lett.* **96**, 111112 (2010).
- <sup>5</sup>B. A. Ruzicka, L. K. Werake, H. Zhao, S. Wang, and K. P. Loh, *Appl. Phys. Lett.* **96**, 173106 (2010).
- <sup>6</sup>J. M. Dawlaty, S. Shivaraman, M. Chandrashekar, F. Rana, and M. G. Spencer, *Appl. Phys. Lett.* **92**, 042116 (2008).
- <sup>7</sup>J. Shang, Z. Luo, C. Cong, J. Lin, T. Yu, and G. G. Gurzadyan, *Appl. Phys. Lett.* **97**, 163103 (2010).
- <sup>8</sup>K. P. Loh, Q. Bao, G. Eda, and M. Chhowalla, *Nat. Chem.* **2**, 1015 (2010).
- <sup>9</sup>G. Eda and M. Chhowalla, *Adv. Mater. (Weinheim, Ger.)* **22**, 2392 (2010).
- <sup>10</sup>Q. L. Bao, H. Zhang, J. X. Yang, S. Wang, D. Y. Tong, R. Jose, S. Ramakrishna, C. T. Lim, and K. P. Loh, *Adv. Funct. Mater.* **20**, 782 (2010).
- <sup>11</sup>Y. P. Wu, B. Wang, Y. F. Ma, Y. Huang, N. Li, F. Zhang, and Y. S. Chen, *Nano Research* **3**, 661 (2010).
- <sup>12</sup>Z. Liu, Q. Liu, Y. Huang, Y. Ma, S. Yin, X. Zhang, W. Sun, and Y. Chen, *Adv. Mater. (Weinheim, Ger.)* **20**, 3924 (2008).
- <sup>13</sup>Z. Luo, P. M. Vora, E. J. Mele, A. T. C. Johnson, and J. M. Kikkawa, *Appl. Phys. Lett.* **94**, 111909 (2009).
- <sup>14</sup>C. H. Lui, K. F. Mak, J. Shan, and T. F. Heinz, *Phys. Rev. Lett.* **105**, 127404 (2010).
- <sup>15</sup>A. Das, S. Pisana, B. Chakraborty, S. Piscanec, S. K. Saha, U. V. Waghmare, K. S. Novoselov, H. R. Krishnamurthy, A. K. Geim, A. C. Ferrari, and A. K. Sood, *Nat. Nanotechnol.* **3**, 210 (2008).
- <sup>16</sup>A. Reina, X. T. Jia, J. Ho, D. Nezich, H. B. Son, V. Bulovic, M. S. Dresselhaus, and J. Kong, *Nano Lett.* **9**, 30 (2009).
- <sup>17</sup>K. S. Subrahmanyam, S. R. C. Vivekchand, A. Govindaraj, and C. N. R. Rao, *J. Mater. Chem.* **18**, 1517 (2008).
- <sup>18</sup>S. Kumar, M. Anija, N. Kamaraju, K. S. Vasu, K. S. Subrahmanyam, A. K. Sood, and C. N. R. Rao, *Appl. Phys. Lett.* **95**, 191911 (2009).
- <sup>19</sup>G. A. Swartzlander, H. Yin, and A. E. Kaplan, *J. Opt. Soc. Am. B* **6**, 1317 (1989).